Supporting Information

Multicolor Room Temperature Phosphorescence in Dibenzothiophene Derivatives-Doped Elastic Binary Polymers for Multi-Step Encryption Displays

Qian Wang,[a] Yan-Yu Xue,[a] Lu-Lu Liu,[a] Fei-Fei Zhao,[a] Yu-Juan Ma,*[a] Jin-Hua Li,*[a] and Guo-Ming Wang[a]

Shandong Provincial Key Laboratory of Intelligent Molecular Science and Engineering, College of Chemistry and Chemical Engineering, Qingdao University, Qingdao, Shandong, 266071, P. R. China
E-mail: jinhuali1978@163.com; mayujuan@qdu.edu.cn.

Supporting Information

Contents

Table S5. The fitting parameters for temperature-dependent phosphorescence lifetimes of TPPTS@PVP@SBR.

Table S6. The fitting parameters for temperature-dependent phosphorescence lifetimes of BZTPA@PVP@SBR.

Table S7. The fitting parameters for temperature-dependent phosphorescence lifetimes of BZNTP@PVP@SBR.

Table S8. The fitting parameters for phosphorescence lifetimes under different strains of TPPTS@PVP@SBR.

Table S9. The fitting parameters for phosphorescence lifetimes over different stretching cycles of TPPTS@PVP@SBR.

Experimental Section

Materials: All chemicals were used without further purification. 4-Dibenzothiophenebronic (TPPTS), Benzo[b]naphtho[1,2-d]thiophene (BZNTP) and Dibenzo[b,d]thiophen-3-aMine (BZTPA), Shanghai Haohong Scientific Co. Ltd; Polyvinyl pyrrolidone (PVP), Shanghai Acmec Biochemical Co. Ltd; Polymerized Styrene Butadiene Rubber (SBR), Shanghai Titan Scientific Co. Ltd; Dichloromethane (CH_2Cl_2), Sinopharm Chemical Reagent Co. Ltd; Rhodamine B (RhB) and ethanol, Sinopharm Chemical Reagent Co. Ltd.

Characterizations and instruments: Room temperature prompt PL spectra were recorded on a Hitachi F-4700 fluorescence spectrometer. Room temperature delayed PLspectra, temperature-dependent PL spectra and all long-lived decay profiles were recorded on an Edinburgh FS5 spectrophotometer. Fluorescence lifetimes were recorded on an Edinburgh FLS1000 spectrophotometer. UV-vis absorption spectra were obtained on a PERSEE TU-1901 spectrophotometer. FT-IR spectra were recorded using a Nicolet is50 IR spectrometer. Typical stress-strain curves were recorded on a YG004 electronic power machine. The Huawei pura 70 and ultraviolet lamp (10 W, 310 nm) were employed to take photographs. Thermogravimetric analysis was carried out using a powder sample with a heating rate of 10 °C K-1 under N2 atmosphere on a NETZSCH STA449 F5 synchronous thermal analyzer. The differential scanning calorimetry data were tested with a Mettler differential scanning calorimetry. Thermogravimetric analysis (TGA) was carried out in the temperature range of 0−480 °C on a TGA 2 thermal analyzer (Mettler-Toledo International Inc) with a heating rate of 5 °C/min. Differential scanning calorimetry (DSC) analysis was performed on a DSC 3 instrument (Mettler-Toledo International Inc) to measure the glass transition temperature (T_g) of the film. All tests were conducted in a nitrogen atmosphere: first, the temperature was raised from −70 °C to 130 °C with a rate of 10 °C/min, maintained for 5 min, and then dropped to −70 ° at the same rate. Next, the sample was heated with a rate of 10 °C/min in the range of −70−130 °C. Dynamic mechanical analysis (DMA) was carried out using a DMA 8000 (Perkin Elmer Instruments). Sample was heated from -115 °C to 50 °C at a rate of 6 °C min^{-1}, with a frequency of 1 Hz. Glass transition temperatures (T_g) are reported as the peak maxima in tan (δ).

Calculation Details: All calculations were carried out using the Gaussian 16 and ORCA 5.0.3 software packages.[1,2] Geometry optimizations of the ground state (S_0), the first excited singlet state (S_1), and the first excited triplet state (T_1) were performed using density functional theory (DFT) and time-dependent density functional theory (TD-DFT) at the PBE0/def2-SVP level.[3,4] Spin-orbit coupling (SOC) matrix elements required for intersystem crossing (ISC) analysis

were calculated using the ORCA package with ZORA scalar relativistic corrections and the ZORA-def2-SVP basis set.[4,5] Wavefunction analyses, including electron–hole distribution and natural transition orbitals, were carried out using Multiwfn.[6] Electron and hole density isosurfaces were visualized using VMD.[7]

[1] M. J. Frisch, G. W. Trucks, H. B. Schlegel, G. E. Scuseria, M. A. Robb, J. R. Cheeseman, G. Scalmani, V. Barone, G. A. Petersson, H. Nakatsuji, X. Li, M. Caricato, A. V. Marenich, J. Bloino, B. G. Janesko, R. Gomperts, B. Mennucci, H. P. Hratchian, J. V. Ortiz, A. F. Izmaylov, J. L. Sonnenberg, Williams, F. Ding, F. Lipparini, F. Egidi, J. Goings, B. Peng, A. Petrone, T. Henderson, D. Ranasinghe, V. G. Zakrzewski, J. Gao, N. Rega, G. Zheng, W. Liang, M. Hada, M. Ehara, K. Toyota, R. Fukuda, J. Hasegawa, M. Ishida, T. Nakajima, Y. Honda, O. Kitao, H. Nakai, T. Vreven, K. Throssell, J. A. Montgomery Jr., J. E. Peralta, F. Ogliaro, M. J. Bearpark, J. J. Heyd, E. N. Brothers, K. N. Kudin, V. N. Staroverov, T. A. Keith, R. Kobayashi, J. Normand, K. Raghavachari, A. P. Rendell, J. C. Burant, S. S. Iyengar, J. Tomasi, M. Cossi, J. M. Millam, M. Klene, C. Adamo, R. Cammi, J. W. Ochterski, R. L. Martin, K. Morokuma, O. Farkas, J. B. Foresman, D. J. Fox, Wallingford, CT, 2016.

[2] F. Neese, F. Wennmohs, U. Becker, C. Riplinger, The ORCA quantum chemistry program package, J. Chem. Phys. 152 (2020) 224108. https://doi.org/10.1063/5.0004608.

[3] C. Adamo, V. Barone, Toward reliable density functional methods without adjustable parameters: The PBE0 model, J. Chem. Phys. 110 (1999) 6158−6170. https://doi.org/10.1063/1.478522.

[4] F. Weigend, R. Ahlrichs, Balanced basis sets of split valence, triple zeta valence and quadruple zeta valence quality for H to Rn: design and assessment of accuracy, Phys. Chem. Chem. Phys. 7 (2005) 3297−3305. https://doi.org/10.1039/B508541A.

[5] D. A. Pantazis; X.-Y. Chen, C. R. Landis, F. Neese, All-electron scalar relativistic basis sets for third-row transition metal atoms, J. Chem. Theory Comput. 4 (208) 908–919. https://doi.org/10.1021/ct800047t.

[6] T. Lu, F. Chen, Multiwfn: a multifunctional wavefunction analyzer, J. Comput. Chem. 33 (2012) 580−592. https://doi.org/10.1002/jcc.22885.

[7] W. Humphrey, A. Dalke, K. Schulten, VMD: visual molecular dynamics, J. Mol. Graph. 14 (1996) 33−38. https://doi.org/10.1016/0263-7855(96)00018-5.

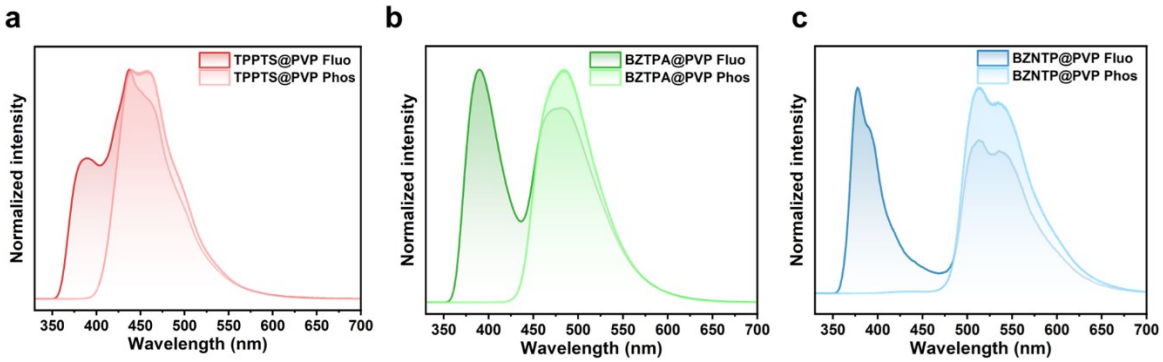

Fig. S1 Prompt and delayed PL emission spectra of TPPTS/BZTPA/BZNTP@PVP films at room temperature.

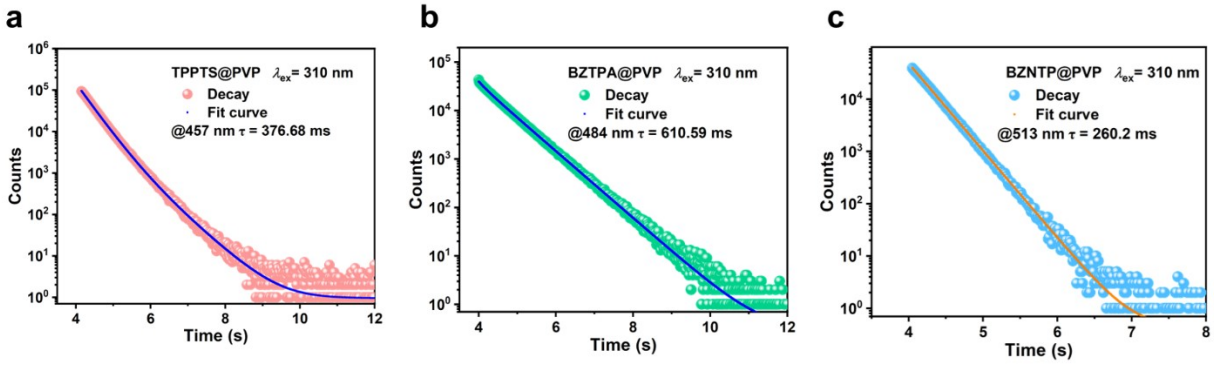

Fig. S2 Long-lived decay curves of TPPTS/BZTPA/BZNTP@PVP films at room temperature.

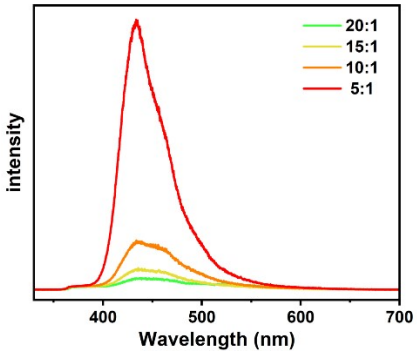

Fig. S3 Delayed PL spectra of TPPTS@PVP@SBR with different polymer ratios.

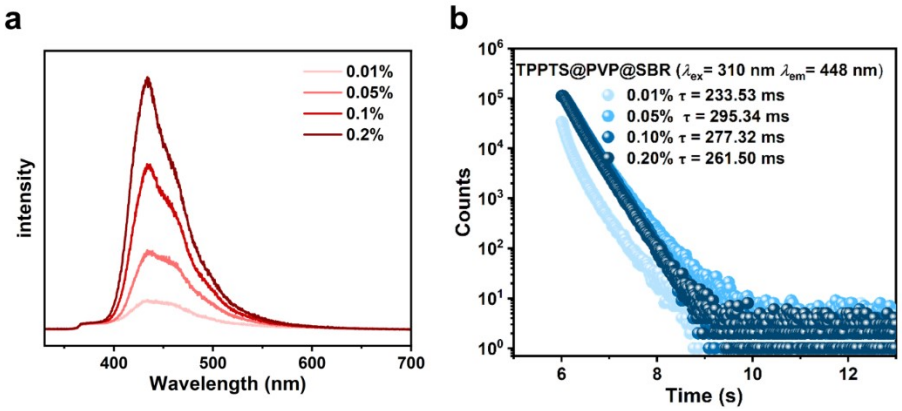

Fig. S4 Delayed PL emission spectra (a) long-lived decay curves (b) of TPPTS@PVP@SBR films with different proportions at room temperature (SBR/PVP=10/1).

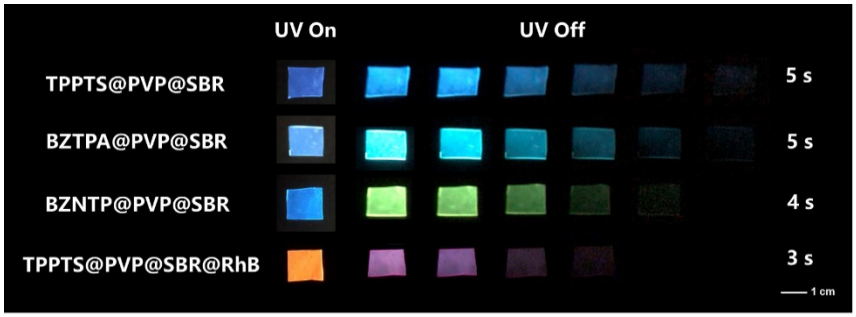

Fig. S5 Photographs for a series of stretchable films before and after removing 310 nm UV lamp.

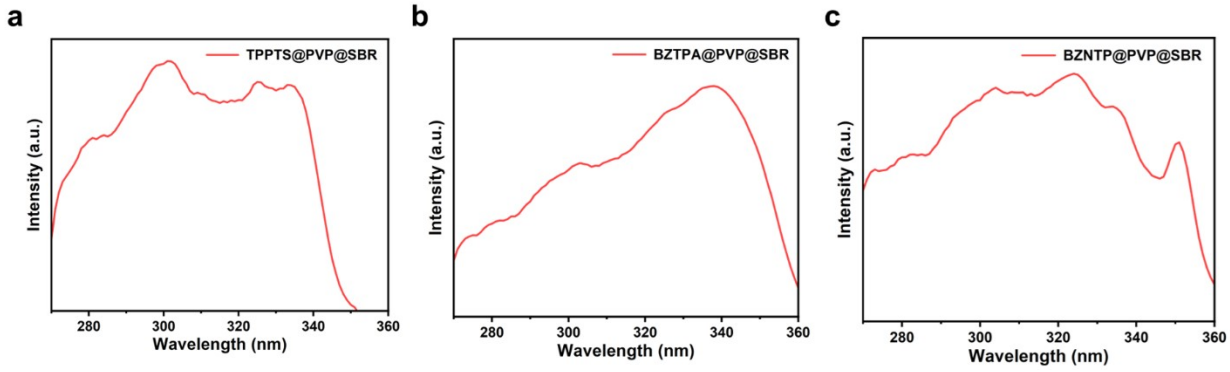

Fig. S6 Prompt PL excitation spectra of TPPTS/BZTPA/BZNTP@PVP@SBR films at room temperature.

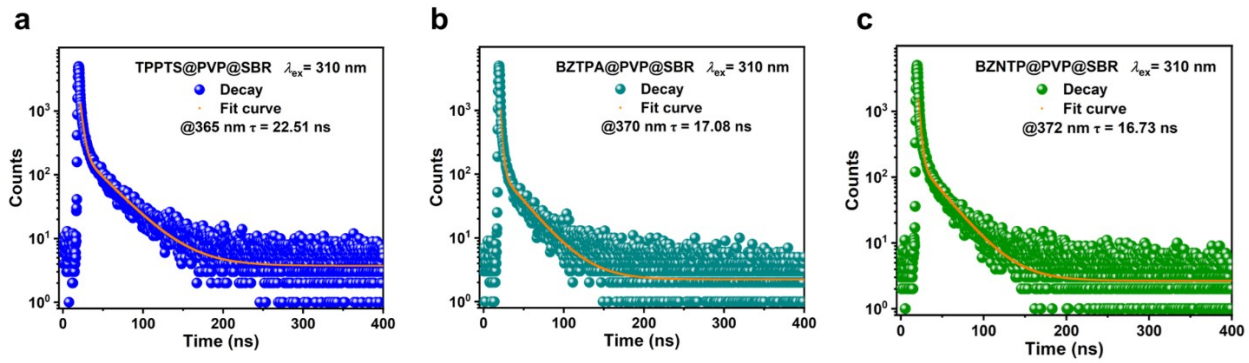

Fig. S7 Fluorescence lifetimes of TPPTS@PVP@SBR, BZTPA@PVP@SBR, and BZNTP@PVP@SBR films at room temperature.

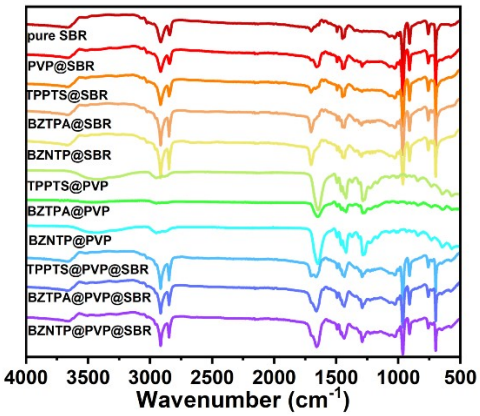

Fig. S8 FT-IR spectra of series doped films.

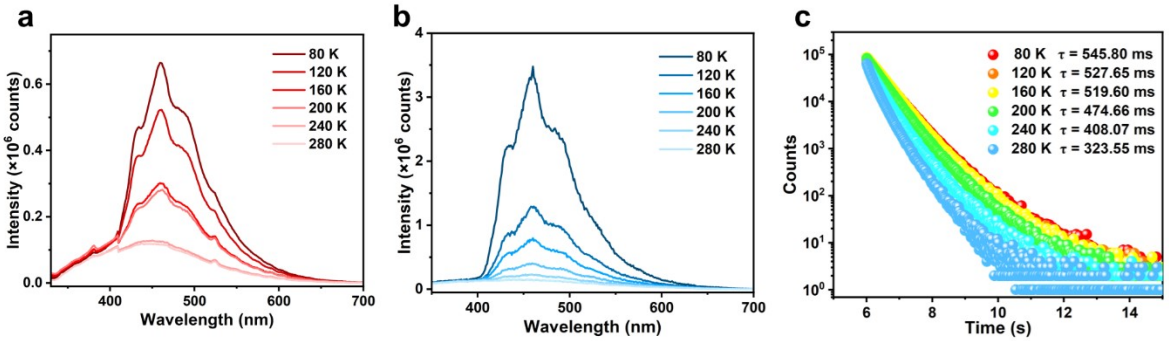

Fig. S9 Temperature-dependent prompt (a) and delayed PL (b) emission spectra and decay curves (c) of TPPTS@PVP@SBR from 80 K to 280 K (λ_{ex} =310 nm).

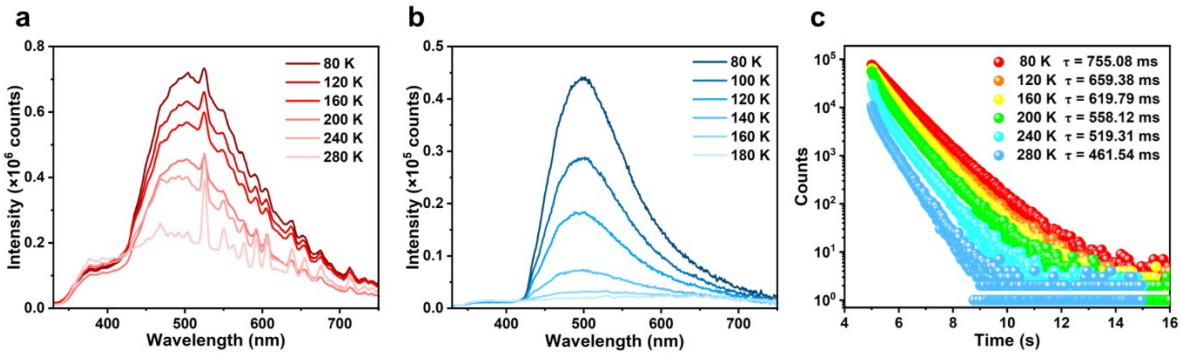

Fig. S10 Temperature-dependent prompt (a) and delayed PL (b) emission spectra and decay curves (c) of BZTPA@PVP@SBR from 80 K to 280 K (λ_{ex} =310 nm).

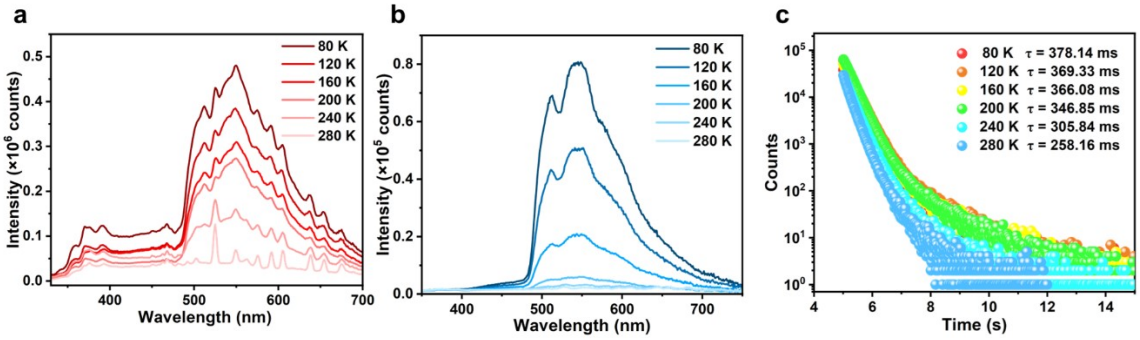

Fig. S11 Temperature-dependent prompt (a) and delayed PL (b) emission spectra and decay curves (c) of BZNTP@PVP@SBR from 80 K to 280 K (λ_{ex} =310 nm).

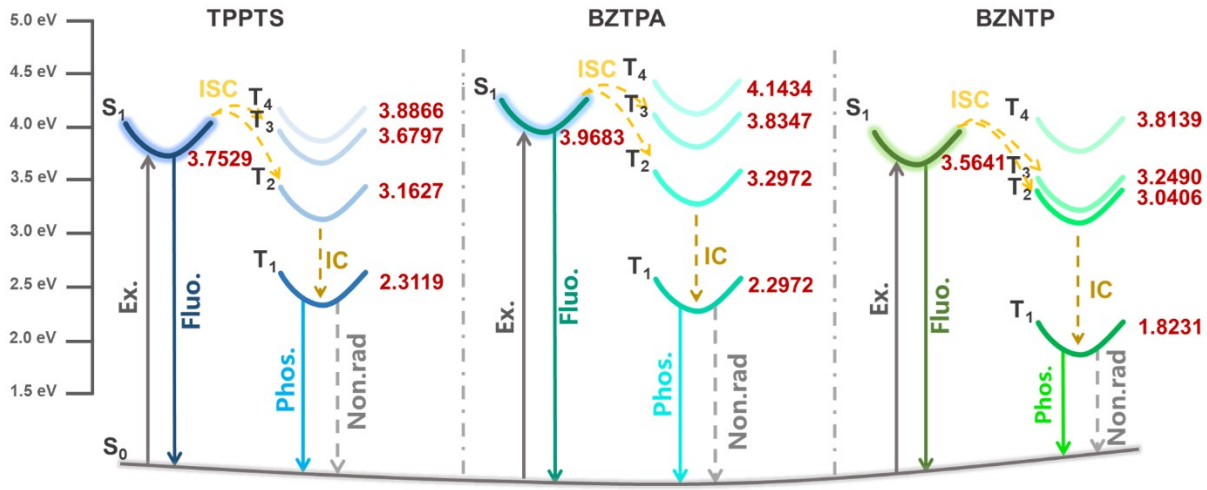

Fig. S12 The excited-state energy level diagrams for TPPTS, BZTPA, and BZNTP molecules.

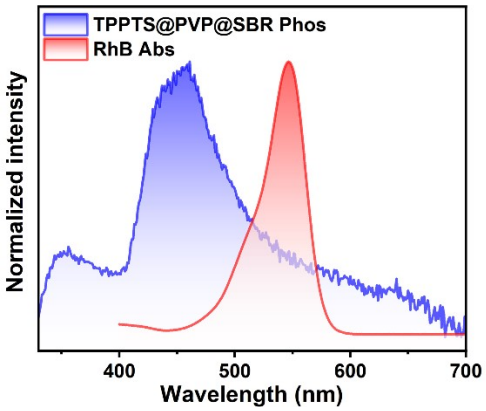

Fig. S13 Delayed emission spectra of TPPTS@PVP@SBR and absorption spectra of RhB.

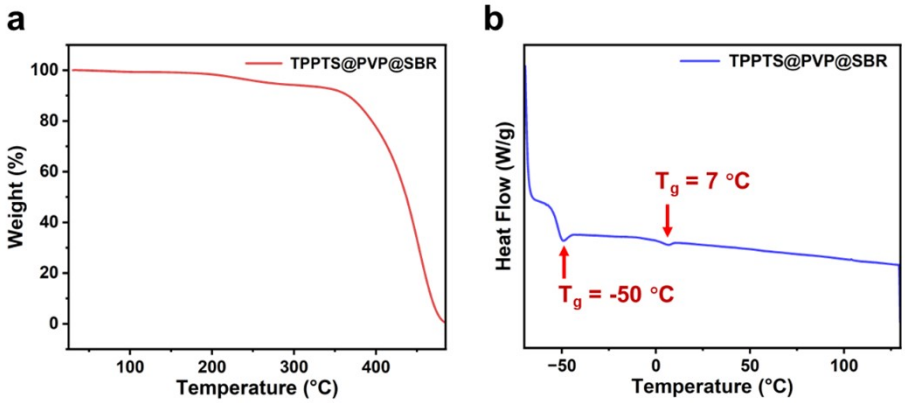

Fig. S14 Thermo-gravimetric analysis (TGA) and differential scanning calorimetry (DSC) traces (second heating curve) for TPPTS@PVP@SBR.

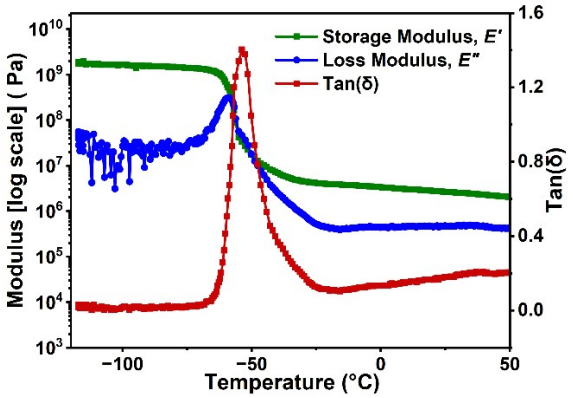

Fig. S15 Dynamic mechanical analysis (DMA) temperature sweeps for TPPTS@PVP@SBR.

Table S1. The fitting parameters for phosphorescence lifetimes of PVP-doped polymer films at room temperature.

Sample	λ_{ex} (nm)	λ_{em} (nm)	τ_1 (ms)	A_1 (%)	τ_2 (ms)	A_2 (%)	$<\tau>$ (ms)	χ^2
TPPTS@PVP	310	457	333.3	81.72	570.6	18.28	376.68	1.3857
BZTPA@PVP		484	206.8	4.54	629.8	95.46	610.59	1.3413
BZNTP@PVP		513	260.2	100	---	---	260.20	1.3459

Table S2. The fitting parameters for phosphorescence lifetimes of TPPTS@PVP@SBR films with different proportions at room temperature.

Sample	λ_{ex} (nm)	λ_{em} (nm)	τ_1 (ms)	A_1 (%)	τ_2 (ms)	A_2 (%)	$<\tau>$ (ms)	χ^2
TPPTS@PVP@SBR-0.01%	310	448	127.5	47.25	328.5	52.75	233.53	1.3211
TPPTS@PVP@SBR-0.05%			252.9	77.28	439.7	22.72	295.34	1.3679
TPPTS@PVP@SBR-0.10%			261.4	75.08	325.3	24.92	277.32	1.2956
TPPTS@PVP@SBR-0.20%			209.7	52.82	319.5	47.18	261.50	1.1749

Table S3. The fitting parameters for fluorescence lifetimes at room temperature.

Sample	λ_{ex} (nm)	λ_{em} (nm)	τ_1 (ns)	A_1 (%)	τ_2 (ns)	A_2 (%)	$<\tau>$ (ns)	χ^2
TPPTS@PVP@SBR	310	365	3.427	36.47	33.46	63.53	22.51	1.3833
BZTPA@PVP@SBR		370	2.085	42.70	28.26	57.30	17.08	1.3989
BZNTP@PVP@SBR		372	2.421	44.13	28.03	55.87	16.73	1.4972

Table S4. The fitting parameters for phosphorescence lifetimes at room temperature.

Sample	λ_{ex} (nm)	λ_{em} (nm)	τ_1 (ms)	A_1 (%)	τ_2 (ms)	A_2 (%)	$<\tau>$ (ms)	χ^2
TPPTS@PVP@SBR	310	448	252.9	77.28	439.7	22.72	295.34	1.3679
BZTPA@PVP@SBR		478	242.4	99.71	1150	0.29	245.03	1.3567
BZNTP@PVP@SBR		513	221.2	96.94	591.3	3.06	232.52	1.4150
TPPTS@PVP@SBR@RhB	310	448	165.8	66.16	315.9	33.84	216.59	1.0118
		590	111.1	58.99	358.6	41.01	212.60	1.3924

Table S5. The fitting parameters for temperature-dependent phosphorescence lifetimes of TPPTS@PVP@SBR.

Temperature (K)	λ_{ex} (nm)	λ_{em} (nm)	τ_1 (ms)	A_1 (%)	τ_2 (ms)	A_2 (%)	<τ> (ms)	χ^2
80	310	448	508.9	93.13	1046	6.87	545.80	1.4042
120			474.6	87.03	883.6	12.97	527.65	1.0696
160			481.8	92.15	963.3	7.85	519.60	1.4151
200			430.6	88.58	816.4	11.42	474.66	1.0077
240			326.0	70.36	602.9	29.64	408.07	1.0008
280			221.0	56.95	459.2	43.05	323.55	1.2066

Table S6. The fitting parameters for temperature-dependent phosphorescence lifetimes of BZTPA@PVP@SBR.

Temperature (K)	λ_{ex} (nm)	λ_{em} (nm)	τ_1 (ms)	A_1 (%)	τ_2 (ms)	A_2 (%)	<τ> (ms)	χ^2
80	310	478	697.6	85.75	1101	14.25	755.08	1.0359
120			354.0	26.82	771.3	73.18	659.38	1.4020
160			465.5	45.13	746.7	54.87	619.79	1.1220
200			300.3	35.56	700.4	64..44	558.12	1.4854
240			198.9	22.83	614.1	77.17	519.31	1.4828
280			133.5	12.36	507.8	87.64	461.54	1.1301

Table S7. The fitting parameters for temperature-dependent phosphorescence lifetimes of BZNTP@PVP@SBR.

Temperature (K)	λ_{ex} (nm)	λ_{em} (nm)	τ_1 (ms)	A_1 (%)	τ_2 (ms)	A_2 (%)	<τ> (ms)	χ^2
80	310	513	340.1	95.90	1268	4.10	378.14	1.1465
120			334.2	96.29	1281	3.71	369.33	1.1374
160			334.8	96.91	1347	3.09	366.08	1.1882
200			311.6	95.87	1165	4.13	346.85	1.4067
240			271.7	90.90	646.9	9.10	305.84	1.0479
280			215.1	82.19	456.9	17.81	258.16	1.2627

Table S8. The fitting parameters for phosphorescence lifetimes under different strains of TPPTS@PVP@SBR.

Strain (%)	λ_{ex} (nm)	λ_{em} (nm)	τ_1 (ms)	A_1 (%)	τ_2 (ms)	A_2 (%)	<τ> (ms)	χ^2
100			211.9	78.64	376.8	21.36	247.12	1.3728
200			97.97	39.79	231.0	60.21	178.07	1.2217
300	310	448	75.47	40.94	197.5	59.06	147.54	1.2698
400			73.06	37.34	181.3	62.66	140.88	1.1705
500			57.22	53.69	207.9	46.31	127.00	0.9396

Table S9. The fitting parameters for phosphorescence lifetimes over different stretching cycles of TPPTS@PVP@SBR.

Times	λ_{ex} (nm)	λ_{em} (nm)	τ_1 (ms)	A_1 (%)	τ_2 (ms)	A_2 (%)	<τ> (ms)	χ^2
10			191.0	64.17	375.7	35.83	257.18	1.2813
20			172.5	55.34	311.3	44.66	234.49	1.1129
30	310	448	110.4	45.24	290.4	54.76	208.97	1.3160
40			90.50	39.82	243.9	60.18	182.82	1.1671
50			88.82	39.28	230.0	60.72	174.54	1.3134